

A NEW THERMODYNAMIC MODEL FOR SOLID METALS UNDER ELASTIC DEFORMATIONS

DALIA S. BERTOLDI AND PABLO OCHOA

ABSTRACT. We present a theoretical model of the free Helmholtz energy (F) for solid metals that incorporates three contributions: the elastic part through a local strain description, the vibrational energy within a quasi-harmonic Einstein model with volume-dependent cohesive energy, and the electronic contribution in the free electron gas setting. To get F , we introduce discrete approximations of the Helmholtz energy defined in cubic lattices and show their convergence to F by finite element methods.

For homogeneous deformations, the obtained model is applied to derive an equation of state (EOS) which shows a very good agreement with experimental data. Moreover, by comparing with other known theoretical EOSs, the present model is highly stable under different estimations of its parameters.

1. INTRODUCTION

Thermostatistical models of matter play a key role in the illustration and understanding of physical behavior of many systems and also in the description of the relations between the properties involved. In fact, the knowledge of the thermal properties and the EOSs of solids is a subject of permanent interest in many fields of basic and applied sciences including physics, metallurgist and geophysics.

There are several experimental, theoretical and numerical approaches to determine EOSs for solids [1, 2, 3, 4, 5, 6, 7, 8, 9]. Among the best-known models, we can be mentioned the ones of Birch-Murnaghan [10], Rose-Vinet [11, 12] and Mie-Grünesisen [13, 14]. Either the EOSs have empirical or theoretical bases they are very useful for interpolation and extrapolation of pressure-volume data, for predicting behaviors and also for determining values of other quantities, as the bulk modulus. However, in most of the standard frameworks, the Helmholtz or Gibbs free energies were not derived, so a full thermodynamic description was not constructed. Moreover, there are many numerical and computational methods such as Molecular Dynamic simulations [15, 16] and density function theory [17, 18] to analyze solids under deformations with a great experimental agreement. Nevertheless, numerical methods can yield isothermal curves for a specific system but, in contrast to analytical approaches, do not provide a full understanding about the mutual relations among physical parameters.

The general purpose of the present work is to contribute to the development of a reference for the study of metal deformations, with a full and self-consistent thermodynamic description. The total free Helmholtz energy is constructed from three contributions: vibrational, electronic and elastic. The vibrational energy is given by a quasi-harmonic Einstein model with a dimensionless cohesive energy versus distance function ($\mathcal{F}(z)$) involving the Wigner-Seitz radius and a material-dependent scaling length, as suggested in classical works by Rose, Ferrante, Smith and collaborators [11, 19]. Secondly, the electronic part is estimated as the energy of free electron gas in the standard form. Finally, the

Date: March 7, 2019.

Key words and phrases.

The second author was partially supported by CONICET and grant PICT 2015-1701 AGENCIA..

elastic energy is described extending the internal energy in a power series with respect to a deformation parameter. This method has been previously used in [20, 21] for describing the behavior of solid argon and gold. However our insight is different, from one side, we explicitly introduce the deformation map u that describes the new positions of the atoms after the deformation, allowing to expand the elastic energy in terms of linear thermal strains. On the other side, we derive a continuum and macroscopic model from a discrete and microscopic description of the atomic interactions. In consequence, our model not only quantifies the change in volume produced by the deformation, but also contemplates how the change in volume is generated.

The paper is organized as follows. In Section 2 we provide the basic setting of the phenomenon under study, including standard assumptions on the partition of the total Helmholtz energy. The construction of the discrete models for the total energy is discussed in Section 3. In this part, we shall also provide full details of the formulation of each discrete energy contribution. The continuum model for the Helmholtz energy, is presented in Section 4. A deep discussion of the model for the case of homogeneous deformations, including derivations of EOSs, is provided in Section 5. In that part, we shall also compare the theoretical findings to both, experimental data and previous equations of state in the literature. In Section 6 we present the general conclusions of the paper. Finally, we close the paper with the Appendix, where we supply the details in deriving the continuum model from the discrete approximations.

2. BASIC FRAMEWORK

We consider a metallic three dimensional body $\Omega_0 \subset \mathbb{R}^3$ with simple cubic structure. We call Ω_0 the initial configuration with temperature T_0 and pressure P_0 . The solid is initially in equilibrium and is deformed into a new stable configuration (Ω) by a change in temperature or pressure. However, we assume that the thermodynamic change does not produce a phase transition.

The total Helmholtz energy of a solid can be expressed as the sum of three terms describing the elastic (F_e), vibrational (F_{vib}) and electronic (F_{el}) contributions [22]:

$$(2.1) \quad F = F_e + F_{el} + F_{vib}.$$

Each of these partial contributions F_i will be found using the following standard expression:

$$(2.2) \quad F_i = E_i - TS_i,$$

where E_i is the internal energy and S_i the corresponding entropy. We shall write each F_i over discretizations of the deformed solid, and then by a limiting procedure we shall derive a continuum model for F .

3. THE DISCRETE MODEL

3.1. Basic considerations.

We model the deformation from Ω_0 onto Ω by a function u with continuous first order partial derivatives. In the sequel, V_0 and V represent the volumes of the initial and final configurations, respectively.

In the initial configuration Ω_0 , we distinguish between the lattice given by the cubic crystal system and the lattices generated by the discretization. The first one is fixed (dashed lines in Fig. 3.1), the nodes of the lattice are all the atoms of the solid and the smallest distance between them is the lattice parameter a . On the other hand, the discretization gives rise to a set of cubic lattices $\Omega_0 \cap \mathcal{L}_h$, where

$\mathcal{L}_h = h\mathbb{Z}^3$ and h is the lattice mesh (solid lines in Fig. 3.1 for $h = 2a$). When $h = a$ the number of nodes ($N_n(h)$) is exactly the number of atoms (N). In the sequel the following parameter will be used:

$$(3.1) \quad N(h) = \begin{cases} N_n(h) & \text{if } h > a, \\ N & \text{if } h \leq a. \end{cases}$$

Moreover, we let u_h the discrete deformation that coincides with u on the nodes of $\mathcal{L}_h \cap \Omega_0$.

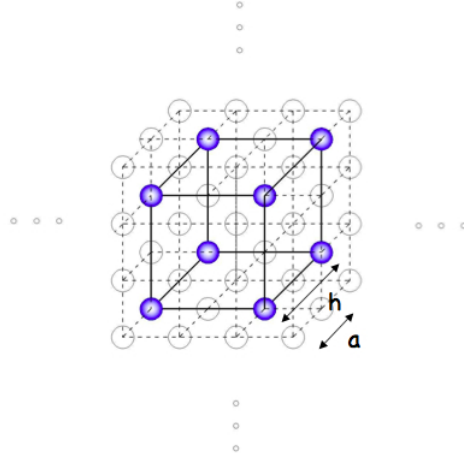


FIGURE 3.1. Representation of the solid with its cubic simple structure with lattice parameter a and its discretization with mesh h .

3.2. Contributions to the discrete total Helmholtz energy.

3.2.1. *Helmholtz elastic energy.* This energy is related to the displacements of the atoms in the deformed configuration with respect to the initial positions, without considering the atomic vibrations. For given h , we will describe the elastic deformation taking into account only the interactions between first-neighbour nodes of the corresponding discretized lattice.

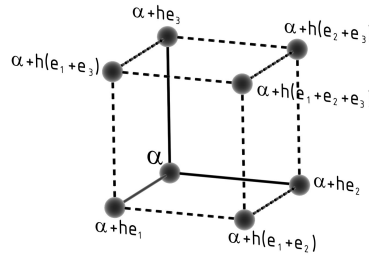


FIGURE 3.2. Representation of a standard lattice cell.

For each h and node $\alpha \in \mathcal{L}_h \cap \Omega_0$, we define the lattice cell as $C_\alpha^h = \alpha + h[0, 1]^3$ (see Fig. 3.2). The internal elastic energy associated to each cell ($E_e^{h,\alpha}$) is considered as the quotient between the total internal energy of the solid and the number of cells (that is approximately $N(h)$). Similarly:

$$V_0 \approx N(h)h^3 \quad \text{and} \quad V \approx \sum_{\alpha \in \mathcal{L}_h \cap \Omega_0} v_\alpha^h$$

where v_α^h is the volume of the deformed lattice cell. Hence, performing a Taylor expansion of $E_e^{h,\alpha}$ around the initial equilibrium state h^3 in terms of v_α^h , we obtain:

$$(3.2) \quad E_e^{h,\alpha} = \frac{\partial E_e^{h,\alpha}}{\partial v_\alpha^h} (v_\alpha^h - h^3) + \frac{1}{2} \frac{\partial^2 E_e^{h,\alpha}}{\partial (v_\alpha^h)^2} (v_\alpha^h - h^3)^2 + \dots = \frac{A}{N(h)} (v_\alpha^h - h^3) + \frac{1}{2} \frac{B}{N(h)h^3} (v_\alpha^h - h^3)^2 + \dots,$$

where B is the Bulk modulus and A the elastic pressure of the solid, both at the initial equilibrium state. In the sequel, we shall re-write (3.2) in terms of bond deformations.

For each lattice cell and for each permutation $\pi \in S_3$ of the elements 1, 2, and 3, the deformation of the edge with endpoints $\alpha + h(e_{\pi(0)} + \dots + e_{\pi(i)})$ and $\alpha + h(e_{\pi(0)} + \dots + e_{\pi(i)} + e_{\pi(i+1)})$ may be quantified by:

$$(3.3) \quad \epsilon_{\alpha,\pi}^{h,i} := \frac{|u_h(\alpha + h(e_{\pi(0)} + \dots + e_{\pi(i)} + e_{\pi(i+1)}) - u_h(\alpha + h(e_{\pi(0)} + \dots + e_{\pi(i)})))|}{h}$$

for $i = 0, 1, 2$ (where we take $\pi(0) = 0$).

The parameter (3.3) characterizes the edge deformation with respect to the reference configuration. Therefore, the term $v_{\alpha,\pi}^{h,i} := h^3 \epsilon_{\alpha,\pi}^{h,i}$ is an approximation of the final cell volume v_α^h . Indeed, an elastic contraction gives rise to $\epsilon_{\alpha,\pi}^{h,i} < 1$ and hence $v_{\alpha,\pi}^{h,i} < h^3$. Similarly, an expansion gives $\epsilon_{\alpha,\pi}^{h,i} > 1$ and $v_{\alpha,\pi}^{h,i} > h^3$. Averaging over all edges and permutations, we get the estimation:

$$(3.4) \quad v_\alpha^h \approx \frac{1}{18} \sum_{\pi,i} v_{\alpha,\pi}^{h,i}.$$

Moreover, observe that the term $v_{\alpha,\pi}^{h,i} - h^3$ is $h^3(\epsilon_{\alpha,\pi}^{h,i} - 1)$ and that $\epsilon_{\alpha,\pi}^{h,i} - 1$ corresponds with the standard linear thermal strain for the edge with endpoints $\alpha + h(e_{\pi(0)} + \dots + e_{\pi(i)})$ and $\alpha + h(e_{\pi(0)} + \dots + e_{\pi(i)} + e_{\pi(i+1)})$.

Plugging the expressions (3.3) and (3.4) into (3.2), we derive:

$$(3.5) \quad E_e^{h,\alpha} \approx \frac{A}{18N} h^3 \sum_{\pi \in S_3} \left[\left(\frac{|u_h(\alpha + h e_{\pi(1)}) - u_h(\alpha)|}{h} - 1 \right) + \left(\frac{|u_h(\alpha + h(e_{\pi(1)} + e_{\pi(2)}) - u_h(\alpha + h e_{\pi(1)})|}{h} - 1 \right) \right. \\ \left. + \left(\frac{|u_h(\alpha + h(e_{\pi(1)} + e_{\pi(2)} + e_{\pi(3)}) - u_h(\alpha + h(e_{\pi(1)} + e_{\pi(2)}))|}{h} - 1 \right) \right] \\ + \frac{B}{36N} h^3 \sum_{\pi \in S_3} \left[\left(\frac{|u_h(\alpha + h e_{\pi(1)}) - u_h(\alpha)|}{h} - 1 \right)^2 + \left(\frac{|u_h(\alpha + h(e_{\pi(1)} + e_{\pi(2)}) - u_h(\alpha + h e_{\pi(1)})|}{h} - 1 \right)^2 \right. \\ \left. + \left(\frac{|u_h(\alpha + h(e_{\pi(1)} + e_{\pi(2)} + e_{\pi(3)}) - u_h(\alpha + h(e_{\pi(1)} + e_{\pi(2)}))|}{h} - 1 \right)^2 \right].$$

Observe that we used the convex approximation $(\sum_i \lambda_i x_i)^2 \approx \sum_i \lambda_i x_i^2$ for $\lambda_i \in [0, 1]$, $\sum_i \lambda_i = 1$ and x_i small.

An approximation to the internal elastic energy of the lattice (E_e^h) will be the sum of (3.5) over inner cells $C_\alpha^h \subset \Omega_0$. On the other hand, the static entropy can be calculated using the formula $S_e^t = -k_B N(h) \sum_i p_i \ln p_i$ with $i = 1, 2$, where $p_1 = q^h = N(h)v/V$ represents the fraction of cell space occupied by nodes of volume v , and $p_2 = 1 - q^h$. Then, using (2.2), the discrete model for the Helmholtz elastic energy of the solid may be written as:

$$(3.6) \quad F_e^h = E_e^h + N(h)Tk_B \left(q^h \ln q^h + (1 - q^h) \ln(1 - q^h) \right).$$

At the initial state, v can be estimated as $4/3\pi(a/2)^3$, where a is the lattice parameter. Then the space filling coefficient when $h = a$ satisfies $q_0 \sim 0.5$ that is expected for cubic simple lattices. Hence

$$q^h \rightarrow q = \frac{q_0 V_0}{V} \quad \text{as } h \rightarrow 0.$$

Observe that $q < 1$ provided $V > 0.5V_0$. This restriction on the deformation will be assumed in the rest of the paper.

A similar equation to (3.2) is obtained in [20, 21] where the internal elastic energy is expanded in terms of the elastic strain $\varepsilon = (V - V_0)/V_0$. However, our approach is different: while ε only quantifies the net change in volume, the strain of the present work (3.3) gives a local description of each edge deformation.

3.2.2. Helmholtz vibrational energy. To describe the vibrational contribution, we treat the atoms as a set of Einstein oscillators [23, 24] in the framework of the quasi-harmonic approximation (QHA). In QHA is assumed that the atomic vibrations are harmonic but the frequency ω depends on V via the following relation [22]:

$$\gamma := -\frac{\partial \ln \omega}{\partial \ln V}.$$

The parameter γ is a kind of Grüneisen parameter [25] that can be taken in a first approximation to be constant. Hence, the above expression can be integrated between two states to obtain:

$$(3.7) \quad \omega = \omega_0 \left(\frac{V_0}{V} \right)^\gamma$$

where ω_0 is the Einstein frequency at the ground state i.e., $T = 0$ and $P = 0$. The correction of the Einstein model presented by equation (3.7) implies that the vibrational energy depends on the deformation via the volume variation.

According to the above considerations, the vibrational contribution to the Helmholtz energy can be expressed as [24]:

$$(3.8) \quad F_{vib}^h = N(h)u_0^h + 3N(h)k_B T \left[\frac{\theta}{2T} + \ln \left(1 - e^{-\theta/T} \right) \right],$$

where $\theta = \hbar\omega(V)/k_B$. The quantity u_0^h is related to the cohesive energy of the solid (E_{coh}) as follows [35]:

$$u_0^h = E_{coh} \mathcal{F}(z_h)$$

with $\mathcal{F}(z_h) = -(1 + z_h)e^{-z_h}$ the standard Rydberg function [12, 19] and z_h a dimensionless variable given as:

$$z_h(V) = (r - r_0)/l,$$

where $r = (3V/(4\pi N(h)))^{1/3}$ is the Wigner-Seitz radius, r_0 is the Wigner-size radius at equilibrium and l is a material-dependent scaling length [19]. We point out that (3.8) contemplates not only the vibrational (kinetic) energy but the static (cohesive) energy as well.

3.2.3. Helmholtz electronic energy. This contribution is estimated as the energy of a standard free electron gas [22, 26]. In this framework, the electronic contribution to the Helmholtz energy can be expressed as [26]:

$$(3.9) \quad F_{el} = \frac{3}{5}n(h)\epsilon_f \left[1 - \frac{5}{12} \left(\frac{\pi k_B T}{\epsilon_f} \right)^2 \right]$$

where ϵ_f is the Fermi energy at the ground state and is defined as [26, 6]:

$$\epsilon_f = \frac{\hbar^2}{2m} \left(3\pi^2 \frac{n(h)}{V_0} \right)^{2/3}.$$

Moreover, $n(h)$ is the number of free electrons and can be taken as:

$$n(h) = N(h) \cdot n_v$$

where n_v is the number of valence electrons per atom.

4. THE CONTINUUM MODEL

The total discrete Helmholtz energy is obtained plugging the contributions (3.6), (3.8) and (3.9) into (2.1), to get:

$$(4.1) \quad \begin{aligned} F_h := & E_e^h + N(h)Tk_B \left(q^h \ln q^h + (1 - q^h) \ln(1 - q^h) \right) \\ & + N(h)E_{coh}\mathcal{F}(z_h) + 3N(h)k_B T \left[\frac{\theta}{2T} + \ln \left(1 - e^{-\theta/T} \right) \right] + \frac{3}{5}n(h)\epsilon_f \left[1 - \frac{5}{12} \left(\frac{\pi k_B T}{\epsilon_f} \right)^2 \right]. \end{aligned}$$

By applying finite element methods and letting $h \rightarrow 0$ in (4.1), we derive a continuum model to the total Helmholtz energy:

$$(4.2) \quad \begin{aligned} F = & \frac{A}{3N} \int_{\Omega_0} \sum_{i=1}^3 (|\partial_i u(x)| - 1) dx + \frac{B}{6N} \int_{\Omega_0} \sum_{i=1}^3 (|\partial_i u(x)| - 1)^2 dx + NTk_B (q \ln q + (1 - q) \ln(1 - q)) \\ & + NE_{coh}\mathcal{F}(z) + 3Nk_B T \left[\frac{\theta}{2T} + \ln \left(1 - e^{-\theta/T} \right) \right] + \frac{3}{5}n\epsilon_f \left[1 - \frac{5}{12} \left(\frac{\pi k_B T}{\epsilon_f} \right)^2 \right], \end{aligned}$$

where

$$(4.3) \quad z = l^{-1} \left[\left(\frac{3V}{4\pi N} \right)^{1/3} - r_0 \right].$$

We refer the reader to the Appendix for the calculations.

Integral representations, as those obtained in (4.2), are usually founded in models for the internal elastic energy (see for example [27, 28] and the references therein). Moreover, the dependence of the elastic part on the gradient of the deformation is also standard in the literature and it accounts for the local deformation at each material point.

Equation (4.2) constitutes our basic model and from it, we can derive a complete thermodynamic description, as we will show in the next section.

5. DISCUSSION AND IMPLICATIONS OF THE MODEL

5.1. Solid without deformation. As a basic example, suppose that the initial conditions of the solid $T_0 = 0$ and $P_0 = 0$ do not change. In this case, the deformation is $u(x, 0, 0) = x$ and its gradient is:

$$\nabla u(x, 0, 0) = \begin{pmatrix} 1 & 0 & 0 \\ 0 & 1 & 0 \\ 0 & 0 & 1 \end{pmatrix}.$$

Thus the elastic contribution in equation (4.2) disappears and the total energy reduces to:

$$F = -NE_{coh} + \frac{3}{5}n\epsilon_f + \frac{3}{2}N\hbar\omega_0.$$

which is the expected Helmholtz energy in the ground state.

5.2. Cubic solid under an homogeneous deformation. Suppose now that we have a cubic solid $[0, s_0]^3$ with initial conditions $V_0 = s_0^3$, T_0 and P_0 . The cube undergoes an homogeneous deformation and it expands at the same rate over the directions e_1 , e_2 and e_3 . A possible form for this deformation is:

$$(5.1) \quad u(x, T, P) = (1 + c(T - T_0) + k(P - P_0))x$$

where c is a constant expressed in K^{-1} and k in $(N/m^2)^{-1}$. Observe that u satisfies the general relation that the standard linear thermal strains over each edge of the cells are proportional to the change in temperature. Below, we present interpretations of the constants c and k .

Recall that the linear thermal expansion coefficient (α_L) at constant pressure ($P = P_0$) can be estimated as:

$$(5.2) \quad \frac{\Delta L}{L_0} = \alpha_L \Delta T,$$

where $\Delta T = T - T_0$, $L_0 = h$ and:

$$\Delta L = |u(\alpha + h(e_{\pi(0)} + \dots + e_{\pi(i)} + e_{\pi(i+1)})) - u(\alpha + h(e_{\pi(0)} + \dots + e_{\pi(i)}))| - h = c\Delta Th.$$

So, we derive:

$$(5.3) \quad \alpha_L = c.$$

A similar relation to (5.3) for the whole solid may be deduced considering the volumetric thermal expansion coefficient (α_V), estimated as:

$$(5.4) \quad \frac{\Delta V}{V_0} = \alpha_V \Delta T.$$

Indeed, using $V_0 = s_0^3$, we have that (5.4) gives:

$$\frac{[(1 + c\Delta T)s_0]^3 - s_0^3}{s_0^3} = \alpha_V \Delta T.$$

A first order Taylor expansion implies:

$$(5.5) \quad c \approx \frac{1}{3} \alpha_V.$$

The approximation (5.5) yields that $\alpha_L \approx (1/3)\alpha_V$, that is a well known result for isotropic materials [26].

Analogously, the isothermal compressibility (κ) can be estimated as:

$$\frac{\Delta V}{V_0} = -\kappa \Delta P$$

where $\Delta P = P - P_0$. In this case:

$$\frac{[(1 + k\Delta P)s_0]^3 - s_0^3}{s_0^3} = -\kappa \Delta T$$

and then the constant k in (5.1) can be interpreted as:

$$k \approx -\frac{1}{3} \kappa.$$

5.2.1. *Helmholtz total energy.* In view of (5.1), we can write:

$$V = (1 + c\Delta T + k\Delta P)^3 V_0.$$

Hence, equation (4.2) gives:

$$(5.6) \quad F = \frac{A}{N} V_0 \left[\left(\frac{V}{V_0} \right)^{1/3} - 1 \right] + \frac{B}{2N} V_0 \left[\left(\frac{V}{V_0} \right)^{1/3} - 1 \right]^2 + NTk_B \left[\frac{V_0}{2V} \ln \left(\frac{V_0}{2V} \right) + \left(1 - \frac{V_0}{2V} \right) \ln \left(1 - \frac{V_0}{2V} \right) \right] \\ + NE_{coh} \mathcal{F}(z) + 3Nk_B T \left[\frac{\theta(V)}{2T} + \ln \left(1 - e^{-\theta(V)/T} \right) \right] + \frac{3}{5} n \epsilon_f \left[1 - \frac{5}{12} \left(\frac{\pi k_B T}{\epsilon_f} \right)^2 \right].$$

Observe that $B/N \sim 10^{-19} - 10^{-18} N/m^2$, $\theta \sim 10^2 - 10^3 K$ [29], $\epsilon_f \sim 10^{-19} J$ [29], and $k_B \sim 10^{-23} J/K$. Since the solid is a unit cube with simple cubic structure, we have $N \sim 10^{30}$. Therefore, (5.6) yields $(\partial^2 F / \partial T^2)_V < 0$ that indicates a thermodynamically stable state.

5.2.2. *Equation of state (EOS).* From equation (5.6) it is possible to obtain a complete description of the thermodynamics of the system. In particular, using the relation $P = -(\partial F / \partial V)_T$, we can get the following equation of state:

$$(5.7) \quad P = -\frac{A}{3N} x^{-2/3} - \frac{B}{3N} \frac{(x^{1/3} - 1)}{x^{2/3}} - \frac{Nk_B T \ln(2x - 1)}{2V_0 x^2} + \frac{3Nk_B \gamma \theta}{V_0} x^{-3} \left(\frac{1}{2} + \frac{1}{e^{\theta/T} - 1} \right) - \frac{E_{coh}}{4\pi l} \left(\frac{4\pi N}{3xV_0} \right)^{2/3} z(x) e^{-z(x)},$$

where $x = V/V_0$ and $z(x)$ is given by (4.3). At the ground state, where $T = 0$ and $P = 0$, equation (5.7) gives:

$$(5.8) \quad \frac{A}{3N} = \frac{3Nk_B\theta\gamma}{2V_0}.$$

Hence, the elastic pressure around the equilibrium cancels out the pressure generated by the atomic vibrations.

Equation (5.7) is easy to implement and the input parameters used to apply it are well known [29, 19]. Moreover, the present theory does not need fitting parameters.

5.2.3. Numerical analysis. In Figure 5.1 we show the agreement between the present EOS (5.7) and the experimental data for Na, Mo and Au. The model is successful in representing the isothermal EOS of the different metals. The values of E_{coh} , B and θ were obtained from [29], whereas l and r_0 from [19]. For simplicity, we take $\gamma = 2$ [26]. For the particular case of Na, we show two different samples, one with $V_0 = 24 \text{ cm}^3/\text{mol}$ ($T = 20 \text{ K}$) and the other with $V_0 = 22.38 \text{ cm}^3/\text{mol}$ ($T = 51 \text{ K}, 150 \text{ K}$ and 250 K).

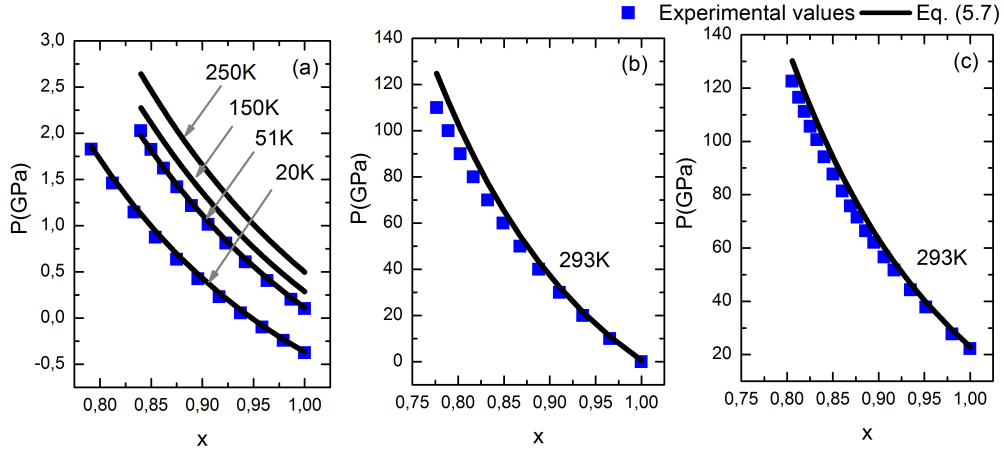


FIGURE 5.1. Relationship between pressure and $x = V/V_0$ for Na (a), Mo (b) and Au (c) at different temperatures. Squares represent experimental values from [30, 31, 32], respectively. The solid lines show the predictions given by eq. (5.7).

Observe that, even do the model was derived from cubic simple lattices, it can be satisfactorily applied to obtain the EOS of bcc and fcc metals. The accuracy is better for small deformations which is consistent with the theoretical approach. Moreover, for highest deformations ($x \approx 0.8$) the relative error between (5.7) and experimental data is 5.9% for Au, 1.6% and 2.5% for Na at $T = 20 \text{ K}$ and $T = 51 \text{ K}$, respectively, and 11.9% for Mo.

In Figure 5.2, we compare (5.7) for Mo with other EOS: Rose-Vinet [22] (in (a)), and Kamal et al. [7] (in (b)). The gray zones represent a probable range of P-V values, considering different estimations of the EOS parameters, viz. B [7, 19, 29, 33] and the pressure derivative of the bulk modulus (B') [7, 19, 34, 35]. These well known models have a sensitive dependence on B' , whose predicted values present a huge relative difference in the literature. On the other hand, the red zone shows the range of P-V given by eq. (5.7) for several values of B [7, 19, 29, 33], θ [29, 36, 37] and E_{coh} [19, 29, 33]. It

is evident that the effect of the parameter variations in our model is much less significant than in the EOSs involving B' .

Based on experimental or numerical P-V values, the usual approach is to treat B' as a fitting parameter. However, when P-V data are not available, Figure 5.2 suggests the use of models not involving B' . In this sense, our framework presents a clear advantage, even for Mo where the agreement is less accurate.

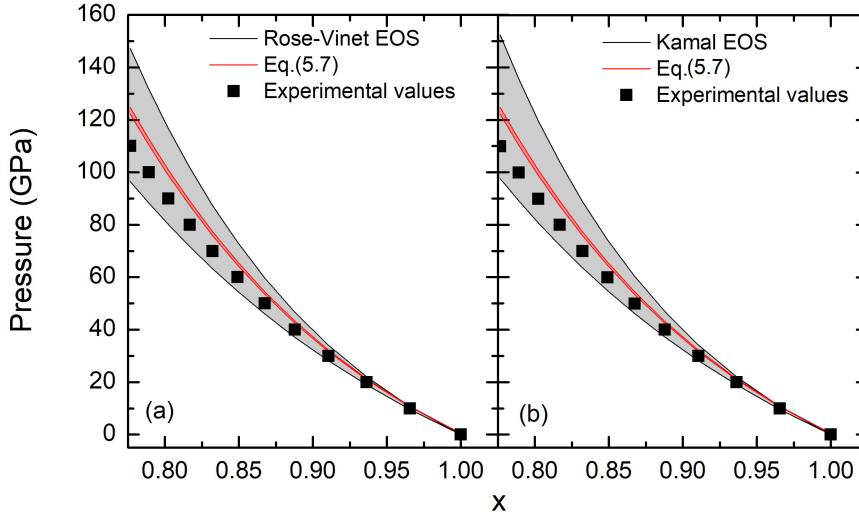


FIGURE 5.2. Comparison of isothermal EOS for Mo at 293 K, obtained from different sources. The shadowed regions represent the range of values in the P-V relation for several estimations of the EOS parameters. The lower curves were obtained by the smallest founded values of B and B' (black curve) and for B , θ and E_{coh} (red curve). Similarly, the upper curves correspond to the highest values.

6. CONCLUDING REMARKS

The main goal of the present paper is to develop a full theoretical description of metallic solids under deformation. This deformation is caused by changes in pressure or temperature and is described in terms of a smooth mapping that connects each point in the initial configuration with its final state.

The model is derived from a discretization of the solid in cubic lattices. On each discrete structure, we consider the total Helmholtz energy as the sum of three contributions: elastic, vibrational and electronic. The elastic part is modelled through a local strain defined in terms of the final distance between first neighbour nodes in the lattice. The vibrational contribution is given by a quasiharmonic Einstein model with a volume-dependent cohesive energy where the Rydberg function intervenes. Lastly, the electronic part is described in the framework of the free electron gas.

From the discrete setting and using finite element method, we obtain the continuum Helmholtz free energy F . The convenience of constructing F is to obtain a complete thermodynamic description, including an equation of state. Hence, it is straightforward to derive other thermodynamic quantities

such as the isobaric thermal expansion ($\alpha_T = -(\partial P/\partial T)_V/V(\partial P/\partial V)_T$) and the heat capacity at constant volume ($C_V = -T(\partial^2 F/\partial T^2)_V$).

The present framework can be applied to any smooth deformation, without phase transitions, and where $V/V_0 > 0.5$. In particular, we make an exhausted analysis in the case of an homogeneous deformation. A comparison with experimental P-V data for Na, Mo and Au, shows that the obtained EOS accounts for the experimental trends at $T \ll T_{melting}$ with a very good agreement. Hence, even do the model is developed from cubic simple lattices, it can be satisfactory applied to other cubic structures. Finally, the present EOS is compared with other known equations of state, concluding that it is more stable under the variations of its parameters. This advantage is due, in part, to the absence of B' .

7. APPENDIX

In this section, we give full details in the derivation of the continuum model (4.2).

7.1. Standard triangulation in \mathbb{R}^3 . Throughout this section, Ω is an open bounded subset of \mathbb{R}^3 . For $s > 0$, we denote:

$$\Omega_s = \{x \in \Omega; \text{dist}(x, \partial\Omega) > s\},$$

where $\text{dist}(x, \partial\Omega)$ stands for the distance of x to the boundary $\partial\Omega$ of the set Ω .

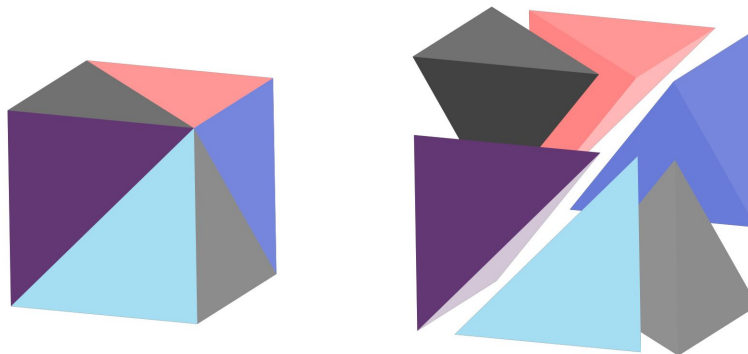


FIGURE 7.1. Triangulation of the cell taking in the standard form.

The standard triangulation of the 3-dimensional cube $C_3 = [0, 1]^3$ is defined as follows (see Fig. 7.1). For all permutations $\pi \in S_3$ of 3 elements, let T^π be the 3-simplex obtained by:

$$T^\pi = \{(x_1, x_2, x_3) \in C_3; x_{\pi(1)} \geq x_{\pi(2)} \geq x_{\pi(3)}\}.$$

Introducing the canonical vectors:

$$e_1 = (1, 0, 0), \quad e_2 = (0, 1, 0), \quad e_3 = (0, 0, 1),$$

we notice that T^π is the convexification of its vertices:

$$T^\pi = \text{conv} \left\{ 0, e_{\pi(1)}, e_{\pi(1)} + e_{\pi(2)}, e_{\pi(1)} + e_{\pi(2)} + e_{\pi(3)} = e_1 + e_2 + e_3 \right\},$$

and that all simplices T^π have 0 and $(1, 1, 1) = e_1 + e_2 + e_3$ as common vertices. The collection of 3! simplices $\{T^\pi\}_{\pi \in S_3}$ constitutes the standard triangulation of C_3 , which can also be naturally extended to each lattice cell $\alpha + hC_3$ where $\alpha \in h\mathbb{Z}^3$:

$$T_\alpha^\pi = \text{conv} \left\{ \alpha, \left\{ \alpha + h \sum_{i=1}^j e_{\pi(i)} \right\}_{j=1}^3 \right\}.$$

Moreover, we call $\mathcal{T}_{h,3}$ the whole triangulation, that is:

$$(7.1) \quad \mathcal{T}_{h,3} = \{T_\alpha^\pi; \alpha \in h\mathbb{Z}^3, \pi \in S_3\}.$$

7.2. The discrete model. Let $U_h \subset \Omega_0$ be the set of those nodes so that the lattice cell C_α^h is included in Ω_0 , and let \mathcal{U}_h be the region covered by those cells. For a given deformation $u \in \mathcal{C}^1(\overline{\Omega_0})$ with continuous first-order derivatives in $\overline{\Omega_0}$, we consider the lattice Helmholtz total energy as:

$$\begin{aligned} F_h := & \sum_{\alpha \in U_h} E_e^{h,\alpha} + N(h)Tk_B \left(q^h \ln q^h + (1 - q^h) \ln(1 - q^h) \right) \\ & + N(h)E_{coh}\mathcal{F}(z) + 3N(h)k_B T \left[\frac{\theta}{2T} + \ln \left(1 - e^{-\theta/T} \right) \right] + \frac{3}{5}n(h)\epsilon_f \left[1 - \frac{5}{12} \left(\frac{\pi k_B T}{\epsilon_f} \right)^2 \right]. \end{aligned}$$

7.3. Integral representation of the elastic contribution. Extend u to the whole space \mathbb{R}^3 so that $u \in \mathcal{C}_0^1(\mathbb{R}^3, \mathbb{R}^3)$. By the fundamental estimate of finite elements [38], the \mathbb{P}_1 -interpolation u_h of u on $\mathcal{T}_{h,3}$, i.e. the continuous function affine on the simplices in $\mathcal{T}_{h,3}$ which coincides with u on $h\mathbb{Z}^3$, satisfies:

$$(7.2) \quad \|u_h - u\|_{W^{1,2}(\Omega)} \rightarrow 0$$

as $h \rightarrow 0$ for any Ω open and smooth domain in \mathbb{R}^3 and moreover:

$$(7.3) \quad \|\nabla u_h\|_{L^\infty(\Omega')} \leq \|u\|_{L^\infty(\Omega')},$$

for all h and bounded set Ω' compactly contained in Ω .

Recalling the expression for the internal elastic energy associated to a cell (3.5) and using the piecewise affine interpolation of u in the triangulation, we may write:

$$\begin{aligned} h^3 \left(\frac{|u_h(\alpha + he_{\pi(1)}) - u_h(\alpha)|}{h} - 1 \right) &= h^3 (|\partial_{\pi(1)} u_h(\alpha)| - 1) = 6 \int_{T_\alpha^\pi} (|\partial_{\pi(1)} u_h(\alpha)| - 1) dx \\ h^3 \left(\frac{|u_h(\alpha + h(e_{\pi(1)} + e_{\pi(2)}) - u_h(\alpha + he_{\pi(1)})|}{h} - 1 \right) &= h^3 (|\partial_{\pi(2)} u_h(\alpha)| - 1) \\ &= 6 \int_{T_\alpha^\pi} (|\partial_{\pi(2)} u_h(\alpha)| - 1) dx, \end{aligned}$$

and finally:

$$\begin{aligned} h^3 \left(\frac{|u_h(\alpha + h(e_{\pi(1)} + e_{\pi(2)} + e_{\pi(3)}) - u_h(\alpha + h(e_{\pi(1)} + e_{\pi(2)}))|}{h} - 1 \right) &= h^3 (|\partial_{\pi(3)} u_h(\alpha)| - 1) \\ &= 6 \int_{T_\alpha^\pi} (|\partial_{\pi(3)} u_h(\alpha)| - 1) dx. \end{aligned}$$

Similarly, we derive integral expressions for the second order terms. Therefore, the discrete model takes the form:

$$\begin{aligned} F_h &= \frac{A}{3N(h)} \int_{\mathcal{U}_h} \sum_{i=1}^3 (|\partial_i u_h(x)| - 1) dx + \frac{B}{6N(h)} \int_{\mathcal{U}_h} \sum_{i=1}^3 (|\partial_i u_h(x)| - 1)^2 dx + N(h) E_{coh} \mathcal{F}(z_h) \\ &\quad + N(h) T k_B (q^h \ln q^h + (1 - q^h) \ln(1 - q^h)) + 3N(h) k_B T \left[\frac{\theta}{2T} + \ln(1 - e^{-\theta/T}) \right] + \frac{3}{5} n(h) \epsilon_f \left[1 - \frac{5}{12} \left(\frac{\pi k_B T}{\epsilon_f} \right)^2 \right]. \end{aligned}$$

7.4. The limiting model. In this part, we shall describe the limit behaviour of the discrete Helmholtz total energy F_h for a given deformation $u \in \mathcal{C}^1(\Omega_0)$.

First, as before, we may consider u as a function in $\mathcal{C}_0^1(\mathbb{R}^3, \mathbb{R}^3)$. In view of the strong convergence (7.2), we derive that:

$$u_h \rightarrow u, \quad \nabla u_h \rightarrow \nabla u \text{ as } h \rightarrow 0,$$

at almost every point in Ω_0 . Call $\chi_h := \chi_{\mathcal{U}^h}$ the characteristic function of the set \mathcal{U}_h . Writing:

$$\int_{\mathcal{U}_h} (|\partial_i u_h(x)| - 1) dx, \quad \int_{\mathcal{U}_h} (|\partial_i u_h(x)| - 1)^2 dx$$

as:

$$\int_{\Omega_0} (|\partial_i u_h(x)| - 1) \chi_h(x) dx, \quad \int_{\Omega_0} (|\partial_i u_h(x)| - 1)^2 \chi_h(x) dx,$$

respectively, and recalling the uniform bound (7.3) of the gradients together with the convergences $|\nabla u_h| \chi_h \nearrow |\nabla u|$ and $|\nabla u_h|^2 \chi_h \nearrow |\nabla u|^2$ as $h \rightarrow 0$, almost everywhere in Ω_0 , we deduce from Lebesgue Dominated Convergence Theorem that:

$$\begin{aligned} (7.4) \quad \lim_{h \rightarrow 0} \left(\frac{A}{3N(h)} \int_{\mathcal{U}_h} \sum_{i=1}^3 (|\partial_i u_h(x)| - 1) dx + \frac{B}{6N(h)} \int_{\mathcal{U}_h} \sum_{i=1}^3 (|\partial_i u_h(x)| - 1)^2 dx \right) \\ = \frac{A}{3N} \int_{\Omega_0} \sum_{i=1}^3 (|\partial_i u(x)| - 1) dx + \frac{B}{6N} \int_{\Omega_0} \sum_{i=1}^3 (|\partial_i u(x)| - 1)^2 dx. \end{aligned}$$

In this way, as h goes to 0, the discrete total Helmholtz energy converges to (4.2).

REFERENCES

- [1] Shanker J, Dulari P and Singh P (2009) Extreme compression behaviour of equations of state. *Physica B: Condensed Matter* **404** 4083.
- [2] Holzapfel W, Hartwig H and Sievers W (2001) Equations of state for Cu, Ag, and Au for wide ranges in temperature and pressure up to 500 GPa and above. *J. Phys. Chem. Ref. Data* **30** 515.
- [3] Alfe D, Vocadlo L, Price G and Gillan M (2004) Melting curve of materials: theory versus experiments. *J. Phys. Condens. Matter* **16** 5973.

- [4] Dewaele A, Torrent M, Loubeyre P and Mezouar M (2008) Compression curves of transition metals in the Mbar range: Experiments and projector augmented-wave calculations. *Phys. Rev. B* **78** 104102.
- [5] Molodets A, Golyshev A and Shakh-ray J (2016) High-pressure high-temperature equations of state of shocked bcc vanadium. *J. of Phys.: Conf. Ser.* **774** 012008.
- [6] Holzapfel W (2001) Equations of state for solids under strong compression. *Crystalline Materials* **216**(9) 473.
- [7] Kapoor K, Kumar A and Dass N (2014) A new temperature-dependent equation of state of solids. *PRAMANA, Journal of Physics* **82** 549.
- [8] Bercegeay C and Bernard S (2005) First-principles equations of state and elastic properties of seven metals. *Phys. Rev. B* **72** 214101.
- [9] Straub G, Aidun J, Wills J, Sanchez-Castro C and Wallace D (1994) Ab initio calculation of melting and thermodynamic properties of crystal and liquid aluminum. *Phys. Rev. B* **50** 5055.
- [10] Birch F (1947) Finite elastic strain of cubic crystals. *Phys. Rev. B* **71** 809.
- [11] Vinet P, Smith J, Ferrante J and Rose J (1987) Temperature effects on the universal equation of state of solids. *Phys. Rev. B* **35** 1945.
- [12] Banerjea A and Smith J (1988) Origins of the universal binding-energy relation. *Phys. Rev. B* **37** 6632.
- [13] Mie G (1903) Zur kinetischen Theorie der einatomigen Körper. *Ann. Phys.* **11** 657.
- [14] Grüneisen M (1912) Theorie des festen Zustandes einatomiger Elemente. *Ann. Phys.* **12** 257.
- [15] Özgen S, Songür L and Kara İ (2012) Equations of state for amorphous and crystalline nickel by means of molecular dynamics method. *Turk. J. Phys.* **36**(1) 59.
- [16] Ono S. (2009) First-principles molecular dynamics calculations of the equation of state for tantalum. *Int. J. Mol. Sci.* **10** 4342.
- [17] Wang H and Lee M (2009) Ab initio calculations of second-, third-, and fourth-order elastic constants for single crystals. *Phys. Rev. B* **79**(22) 224102.
- [18] Ravindran P, Fast L, Korzhavyi P, Johansson L, Wills J, and Eriksson O (1988) Density functional theory for calculation of elastic properties of orthorhombic crystals: Application to TiSi₂. *J. Appl. Phys.* **84**(9) 4891.
- [19] Rose J, Smith J, Guinea F and Ferrante J (1984) Universal features of the equation of state of metals. *Phys. Rev. B* **29**(6) 2963.
- [20] Balcerzak T, Szalowski K and Jaščur M (2010) A simple thermodynamic description of the combined Einstein and elastic models. *J. Phys. Condens. Matter* **22**(42) 401.
- [21] Balcerzak T, Szalowski K and Jaščur M (2014) A self-consistent thermodynamic model of metallic systems. Application for the description of gold. *J. Appl. Phys.* **116**(4) 043508.
- [22] Grimvall G (1999) *Thermophysical properties of materials* Elsevier.
- [23] Hill T (1960) *An introduction to Statistical thermodynamics* Addison-Wesley Series in Chemistry, Dover.
- [24] Hudson J (1996) *Thermodynamics of materials* John Wiley and Son.
- [25] Bertoldi D, Miranda E and Guillermet, A (2014) Revisiting the thermostatics of the Grüneisen parameters and applications to quasiharmonic solids. *J. Phys. Chem. Solids* **75**(10) 1147.
- [26] Girifalco L (2000) *Statistical mechanics of solids* Oxford University Press.
- [27] Ciarlet P (2008) *Differential geometry: theory and applications* CAM **8**.
- [28] Dimitrienko Y (2011) *Nonlinear Continuum Mechanics and Large Inelastic Deformations* Germany: Springer.
- [29] Kittel C (2004) *Introduction to Solid State Physics* Wiley.
- [30] Beecroft R and Sewnson C (1961) An experimental equation of state for sodium. *J. Phys. Chem. Solids* **18**(4) 329.
- [31] Takemura K and Dewaele A (2008) Isothermal equation of state for gold with a He-pressure medium. *Phys. Rev. B* **78**(10) 104119.
- [32] Hixson R and Fritz J (1992) Shock compression of tungsten and molybdenum. *J. Appl. Phys.* **71**(4) 17.
- [33] Ratanaphan S, Olmsted D, Bulatov V (2015) Grain boundary energies in body-centered cubic metals. *Acta Mater.* **88** 346.
- [34] Raju S, Mohandas E and Raghunathan V (1997) The pressure derivative of bulk modulus of transition metals: an estimation using the method of model potentials and a study of the systematics. *J. Phys. Chem. Solids* **58**(9) 1367.
- [35] Bertoldi D, Ramos S and Guillermet A (2017) Interrelations between EOS parameters and cohesive energy of transition metals: Thermostatistical approach, ab initio calculations and analysis of universality features. *J. Phys. Chem. Solids* **107** 93.
- [36] Tari A (2003) *The specific heat of matter at low temperatures* Imperial Coll.
- [37] Killean R and Lisher E (1975) The Debye temperatures of the face centred cubic metals. I. X-ray and neutron diffraction results. *J. Phys. F: Met. Phys.* **5** 1107.

[38] Ciarlet P (2002) *The finite element method for elliptic problems* **40** (SIAM) Philadelphia.

D. S. BERTOLDI, UNIVERSIDAD NACIONAL DE CUYO, 5500 MENDOZA, ARGENTINA

E-mail address: `daliasurena_ber@hotmail.com`

P. OCHOA, UNIVERSIDAD NACIONAL DE CUYO-CONICET, 5500 MENDOZA, ARGENTINA

E-mail address: `ochopablo@gmail.com`